JOC Article

Kinetic Investigations of the Process of Encapsulation of Small Hydrocarbons into a Cavitand−Porphyrin

Jun Nakazawa,[†] Yoshitake Sakae,[§] Misako Aida,[§,⊥] and Yoshinori Naruta*[,†,‡]

Graduate School of Sciences and Institute for Materials Chemistry and Engineering (IMCE), Kyushu University, 6-10-1 Hakozaki, Higashi-ku, Fukuoka, Japan, and Graduate School of Science, Center for Quantum Life Sciences (QLiS), and Department of Chemistry, Hiroshima University, 1-3-1 Kagamiyama, Higashi-Hiroshima, Japan

naruta@ms.ifoc.kyushu-u.ac.jp

Received June 19, 2007

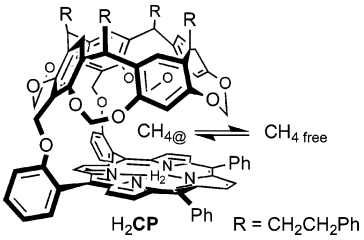

Exchange of guest molecules into capsule shaped host molecules is the most fundamental process in host−guest chemistry. Several examples of quantitative measurements of guest exchange rates have been reported. However, there have been no reports on the activation energies of these processes. A molecule known as cavitand−porphyrin (H_2**CP**) has been reported to have a flexible host structure capable of facilitating moderate guest exchange rates suitable for kinetic measurements of the guest exchange process with ^{1}H NMR. In this article, various kinetic and thermodynamic parameters related to the process of encapsulation of small hydrocarbons into H_2**CP** in $CDCl_3$ solution were determined by 2D exchange spectroscopy (EXSY): association and dissociation rate constants ($k_{ass} = 320$ M^{-1} s^{-1}, $k_{diss} = 1.4$ s^{-1} for methane at 25 °C), the corresponding activation energies ($E_{a,ass} = 27$ kJ·mol^{-1}, $E_{a,diss} = 58$ kJ·mol^{-1}), and thermodynamic parameters for each process ($\Delta G^{\ddagger}_{ass} = 59$ kJ·mol^{-1}, $\Delta G^{\ddagger}_{diss} = 72$ kJ·mol^{-1}, $\Delta H^{\ddagger}_{ass} = 25$ kJ·mol^{-1}, $\Delta H^{\ddagger}_{diss} = 55$ kJ·mol^{-1}, $\Delta S^{\ddagger}_{ass} = -113$ J·K^{-1}·mol^{-1}, and $\Delta H^{\ddagger}_{diss} = 58$ J·K^{-1}·mol^{-1} for methane). The thermodynamic parameters ($\Delta G° = -13$ kJ·mol^{-1}, $\Delta H° = -31$ kJ·mol^{-1}, $\Delta S° = -60$ J·K^{-1}·mol^{-1} for methane) for this encapsulation equilibrium determined by EXSY were comparable to those for methane determined by 1D ^{1}H NMR titration ($\Delta G° = -11$ kJ·mol^{-1}, $\Delta H° = -33$ kJ·mol^{-1}, $\Delta S° = -75$ J·K^{-1}·mol^{-1} for methane). In addition, the structure of the methane encapsulation process was revealed by ab initio MO calculations. The activation energies for methane association/dissociation were estimated from MP2 calculations ($E_{a,ass} = 58.3$ kJ·mol^{-1}, $E_{a,diss} = 89.1$ kJ·mol^{-1}, and $\Delta H° = -30.8$ kJ·mol^{-1}). These values are in accord with the experimentally determined values. The observed guest exchange rates and energies are compared with the corresponding values of various reported capsule-shaped hosts.

Introduction

In molecular recognition chemistry, many examples of chemoselective recognition with use of various strong interactions between hosts and guests have been reported.[1] Examples include metal ion recognition within crown ethers by preorganized macrocyclic coordination environments, and nucleoside recognition with complementary base pairs by multi-hydrogen-bonding interactions. On the other hand, development of host systems capable of molecular recognition of hydrocarbon

* Address correspondence to this author. Fax: 81 092 642 2715. Phone: 81 092 642 2731.
[†] Graduate School of Sciences, Kyushu University.
[‡] Institute for Materials Chemistry and Engineering, Kyushu University.
[§] Graduate School of Science, Hiroshima University.
[⊥] Center for Quantum Life Sciences and Department of Chemistry, Hiroshima University.

(1) (a) Lehn, J. -M. *Supramolecular Chemistry. Concepts and Perspectives*; VCH: Weinheim, Germany, 1995. (b) Rudkevich, D. M. *Angew. Chem.* **2004**, *116*, 568; *Angew. Chem., Int. Ed.* **2004**, *43*, 558.

10.1021/jo701299v CCC: $37.00
Published on Web 11/03/2007

molecules, especially for small molecules such as methane, has been proven difficult to achieve with use of host molecules having a simple recognition site,[2] because of the lack of strong interactions between host and guest molecules. This feature of hydrocarbons makes their selective recognition less efficient. Thus, for the binding of hydrocarbon guest molecules, capsule-like hosts must sterically and dynamically entrap the guest molecule into the host. Over the past two decades, there have been reports of hydrocarbon recognition by capsule-shaped hosts having a hydrophobic cavity with a specific shape and a limited volume for selective encapsulation.[3] These molecular capsules have attracted interest with regard to their applications as "flasks" for molecular storage, separation tools, sensors, and catalysts for specific chemical reactions.[1,2i,4]

A variety of capsule-like compounds have been reported[5] including covalently linked compounds[3b,c,e,f,6] and compounds that are self-assembled by metal coordination[7] or hydrogen-bonding interactions.[8] Covalently linked capsules such as "carcerands" typically have rigid enclosed structures.[6a] The high structural stability of covalently linked capsules is the most advantageous reason for using them as catalysts relative to other capsules made by hydrogen-bonding or coordinating interactions. However, this structural stability is not suitable for release or exchange of encapsulated guest molecules. For example, reversible recognition of small hydrocarbons, such as methane, by carcerands has not yet been achieved. To use covalently linked capsules as catalysts of encapsulated guest molecules, the capsule requires a flexible portal for guest exchange. The capsules called "hemi-carcerands" satisfy this requirement by having fewer linkers connecting the two cavitand hemispheres to increase the portal flexibility.[6b,c] Carcerands typically have 4 linkers while hemi-carcerands have 2 to 3 linkers

SCHEME 1. Encapsulation of Small Hydrocarbons into Free-Base Cavitand−Porphyrin (R = −CH_2CH_2Ph)[a]

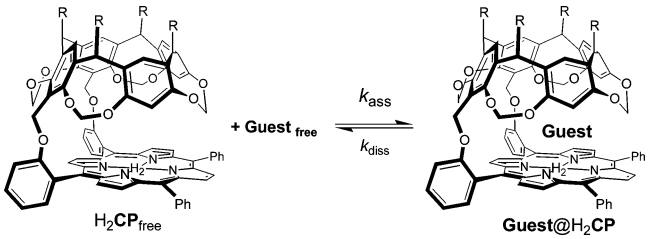

[a] Applied guests in this article are methane, acetylene, and ethylene.

We reported syntheses and small hydrocarbon encapsulations of "cavitand−porphyrin" hosts in previous articles.[9] The covalent-bonding-type H_2**CP** host has a limited-volume cavity for encapsulation of small hydrocarbons such as methane and ethane. To accommodate small guest molecules and to retain suitable flexibility of its portal, a cavitand and a porphyrin are connected by two ether linkages. H_2**CP** is capable of encapsulation of a single guest molecule smaller than propane and encapsulated guest molecules undergo facile exchange with guest molecules in bulk solution (Scheme 1). H_2**CP** demonstrates size-selective and reversible encapsulation of small hydrocarbons within the host cavity. In addition, the porphyrin can function not only as the bottom of the H_2**CP** capsule but also as a potential catalyst.

Guest size selectivity[10] and the ability to retain guest molecules are important attributes for development of host molecules as sensors and as a means for molecular storage, as well as for development of further chemical reactions within the capsules. Guest retention time is generally affected by the shape of the capsule portal as well as the affinity of the guest for the cavity. This can be evaluated by examining the rate constants for guest association/dissociation. However, a comprehensive and systematic kinetic study has yet to be carried out. Reports on exchange rates and activation energies for capsule-shaped host and small guest systems are lacking relative

(2) (a) Cram, D. J. *Nature* **1992**, *356*, 29. (b) Timmerman, P.; Verboom, W.; Reinhoudt, D. N. *Tetrahedron* **1996**, *52*, 2663. (c) Rebek, J., Jr. *Chem. Commun.* **2000**, 637. (d) Rebek, J., Jr. *Angew. Chem.* **2005**, *117*, 2104; *Angew. Chem., Int. Ed.* **2005**, *44*, 2068. (e) Gibb, B. C. *J. Supramol. Chem.* **2002**, *2*, 123. (f) Vriezema, D. M.; Aragonès, M. C.; Elemans, J. A. A. W.; Cornelissen, J. J. L. M.; Rowan, A. E.; Nolte, R. J. M. *Chem. Rev.* **2005**, *105*, 1445. (g) Rudkevich, D. M. *Bull. Chem. Soc. Jpn.* **2002**, *75*, 393. (h) Hof, F.; Craig, S. L.; Nuckolls, C.; Rebek, J., Jr. *Angew. Chem.* **2002**, *114*, 1556; *Angew. Chem., Int. Ed.* **2002**, *41*, 1488. (i) Purse, B. W.; Rebek Jr., J. *Proc. Natl. Acad. Sci. U.S.A.* **2005**, *102*, 10777.

(3) (a) Branda, N.; Wyler, R.; Rebek, J., Jr. *Science* **1994**, *263*, 1267. (b) Paek, K.; Ihm, C.; Ihm, H. *Tetrahedron Lett.* **1999**, *40*, 4697. (c) Paek, K.; Cho, J. *Tetrahedron Lett.* **2001**, *42*, 1927. (d) Shivanyuk, A.; Scarso, A.; Rebek, J., Jr. *Chem. Commun.* **2003**, *11*, 1230. (e) Jasat, A.; Sherman, J. C. *Chem. Rev.* **1999**, *99*, 931. (f) Middel, O.; Verboom, W.; Reinhoudt, D. N. *J. Org. Chem.* **2001**, *66*, 3998. (g) Starnes, S. D.; Rudkevich, D. M.; Rebek, J., Jr. *J. Am. Chem. Soc.* **2001**, *123*, 4659. (h) Kuroda, Y.; Hiroshige, T.; Sera, T.; Shiroiwa, Y.; Tanaka, H.; Ogoshi, H. *J. Am. Chem. Soc.* **1989**, *111*, 1912. (i) Elemans, J. A. A. W.; Claase, M. B.; Aarts, P. P. M.; Rowan, A. E.; Schenning, A. P. H. J.; Nolte, R. J. M. *J. Org. Chem.* **1999**, *64*, 7009. (j) Letzel, M. C.; Decker, B.; Rozhenko, A. B.; Schoeller, W. W.; Mattay, J. *J. Am. Chem. Soc.* **2004**, *126*, 9669. (k) Yoshizawa, M.; Tamura, M.; Fujita, M. *J. Am. Chem. Soc.* **2004**, *126*, 6846. (l) Kobayashi, K.; Ishii, K.; Sakamoto, S.; Shirasaka, T.; Yamaguchi, K. *J. Am. Chem. Soc.* **2003**, *125*, 10615. (m) Chapman, R. G.; Sherman, J. C. *J. Am Chem. Soc.* **1998**, *120*, 9818.

(4) Yoshizawa, M.; Miyagi, S.; Kawano, M.; Ishiguro, K.; Fujita, M. *J. Am. Chem. Soc.* **2004**, *126*, 9172.

(5) (a) Corbellini, F.; Fiammengo, R.; Timmerman, P.; Crego-Calama, M.; Versluis, K.; Heck, A. J. R.; Luyten, I.; Reinhoudt, D. N. *J. Am. Chem. Soc.* **2002**, *124*, 6569. (b) Zadmard, R.; Junkers, M.; Schrader, T.; Grawe, T.; Kraft, A. *J. Org. Chem.* **2003**, *68*, 6551. (c) Fiammengo, R.; Timmerman, P.; Huskens, J.; Versluis, K.; Heck, A. J. R.; Reinhoudt, D. N. *Tetrahedron* **2002**, *58*, 757.

(6) (a) Cram, D. J.; Karbach, S.; Kim, Y. H.; Baczynskyj, L.; Marti, K.; Sampson, R. M.; Kalleymeyn, G. W. *J. Am. Chem. Soc.* **1988**, *110*, 2554. (b) Cram, D. J.; Tanner, M. E.; Knobler, C. B. *J. Am. Chem. Soc.* **1991**, *113*, 7717. (c) Leontiev, A. V.; Rudkevich, D. M. *Chem. Commun.* **2004**, 1468. (d) Cram, D. J.; Blanda, M. T.; Paek, K.; Knobler, C. B. *J. Am. Chem. Soc.* **1992**, *114*, 7765. (e) Garel, L.; Dutasta, J.-P.; Collet, A. *Angew. Chem.* **1993**, *105*, 1249; *Angew. Chem., Int. Ed. Engl.* **1993**, *32*, 1169. (f) Kobayashi, N.; Mizuno, K.; Osa, T. *Inorg. Chim. Acta* **1994**, *224*, 1. (g) Iwamoto, H.; Yukimasa, Y.; Fukazawa, Y. *Tetrahedron Lett.* **2002**, *43*, 8191. (h) Ihm, C.; In, Y.; Park, Y.; Peak, K. *Org. Lett.* **2004**, *6*, 369.

(7) (a) Fochi, F.; Jacopozzi, P.; Wegelius, E.; Rissanen, K.; Cozzini, P.; Marastoni, E.; Fisicaro, E.; Manini, P.; Fokkens, R.; Dalcanale, E. *J. Am. Chem. Soc.* **2001**, *123*, 7539. (b) Yamanaka, M.; Yamada, Y.; Sei, Y.; Yamaguchi, K.; Kobayashi, K. *J. Am. Chem. Soc.* **2006**, *128*, 1531. (c) Fujita, M.; Oguro, D.; Miyazaka, M.; Oka, H.; Yamaguchi, K.; Ogura, K. *Nature* **1995**, *378*, 469. (d) Baldini, L.; Ballester, P.; Casnati, A.; Gomila, R. M.; Hunter, C. A.; Sansone, F.; Ungaro, R. *J. Am. Chem. Soc.* **2003**, *125*, 14181.

(8) (a) Tucci, F. C.; Renslo, A. R.; Rudkevich, D. M.; Rebek, J., Jr. *Angew. Chem.* **2000**, *112*, 1118; *Angew. Chem., Int. Ed.* **2000**, *39*, 1076. (b) Heinz, T.; Rudkevich, D. M.; Rebek, J., Jr. *Nature* **1998**, *394*, 764. (c) Kobayashi, K.; Shirasaka, T.; Yamaguchi, K.; Sakamoto, S.; Horn, E.; Furukawa, N. *Chem. Commun.* **2000**, 41. (d) Kobayashi, K.; Ishii, K.; Yamanaka, M. *Chem. Eur. J.* **2005**, *11*, 4725. (e) Arai, S.; Ohkawa, H.; Ishihara, S.; Shibue, T.; Takeoka, S.; Nishide, H. *Bull Chem. Soc. Jpn.* **2005**, *78*, 2007. (f) Mogck, O.; Pons, M.; Böhmer, V.; Vogt, W. *J. Am. Chem. Soc.* **1997**, *119*, 5706. (g) Cave, G. W. V.; Antesberger, J.; Barbour, L. J.; McKinlay, R. M.; Atwood, J. L. *Angew. Chem.* **2004**, *116*, 5375; *Angew. Chem., Int. Ed.* **2004**, *43*, 5263. (h) Palmer, L. C.; Rebek, J., Jr. *Org. Lett.* **2005**, *7*, 787.

(9) (a) Nakazawa, J.; Hagiwara, J.; Mizuki, M.; Shimazaki, Y.; Tani, F.; Naruta, Y. *Angew. Chem.* **2005**, *117*, 3810; *Angew. Chem., Int. Ed.* **2005**, *44*, 3744. (b) Nakazawa, J.; Hagiwara, J.; Mizuki, M.; Shimazaki, Y.; Tani, F.; Naruta, Y. *Bull. Chem. Soc. Jpn.* **2006**, *79*, 1431. (c) Nakazawa, J.; Mizuki, M.; Shimazaki, Y.; Tani, F.; Naruta, Y. *Org. Lett.* **2006**, *8*, 4275.

(10) Mecozzi, S.; Rebek, J., Jr. *Chem. Eur. J.* **1998**, *4*, 1016.

TABLE 1. The Association Constants and Thermodynamic Parameters of Encapsulation of Small Hydrocarbons into H_2CP Obtained by 1D-^{1}H NMR in $CDCl_3$[a]

	CH_4@H_2**CP**	C_2H_2@H_2**CP**	C_2H_4@H_2**CP**
K (M^{-1})[b]	81	130	49
$\Delta G°$ ($kJ\cdot mol^{-1}$)[c]	−10.9	−12.1	−9.7
$\Delta H°$ ($kJ\cdot mol^{-1}$)[d]	−33	−33	−29
$\Delta S°$ ($J\cdot K^{-1}\cdot mol^{-1}$)[e]	−75	−71	−66

[a] [H_2**CP**$_{total}$] = 5 mM. Estimated error range: K, <10%; $\Delta G°$, <5%; $\Delta H°$, <10%; $\Delta S°$, <20%. [b] K = ([Guest$_@$])/([H_2**CP**$_{free}$] × [Guest$_{free}$]), at 25 °C. [c] $\Delta G° = -RT \ln K$. [d] Obtained by van't Hoff plots in the range of 25−45 °C. [e] $\Delta S° = -(\Delta G° - \Delta H°)/T$.

to guest selectivity studies.[3m,6b,8f,11] In most examples reported thus far, small guest exchange rates between a capsule and bulk solution have been compared only with signal-coalescence time scale measurements obtained from the signal shapes in ^{1}H NMR spectra.[3b,c,6c,h]

The lack of kinetic studies on hydrocarbon guest exchange is due to the lack of applicable experimental methods: NMR is a practically useful tool only for observing reversible processes in host−guest systems, though the observable range of rates is significantly affected by the experimental parameters of spin relaxation time, shimming time, and applied temperature, among others.[6b,d,e,12] Even if guest exchange rates in an objective host−guest system are within the observable range, this method is challenging to apply to hosts self-assembled through hydrogen-binding and coordination chemistry, due to exchange of host components as well as guest exchange. This makes the kinetic analyses complicated. Since each previously published report uses a different guest molecule, straightforward conclusions cannot be drawn. However, the combination of these reports provides insights into intrinsic kinetic characteristics of the guest exchange process.

Fortunately, we can observe the process of exchange and encapsulation of small hydrocarbons into H_2**CP** by exchange spectroscopy (EXSY, an NMR magnetization exchange method) because the exchange rates are close to the spin relaxation time.[12] Using the observed exchange rates, we compared guest exchange rates with other capsule-shaped hosts. These kinetic and thermodynamic data will contribute to the design of molecular catalysts, which will allow conversions of encapsulated guests within the cavities.

Results and Discussions

Thermodynamic and Kinetic Data Obtained from 1D-^{1}H NMR. As reported in our previous articles,[9] ^{1}H NMR spectra of H_2**CP** with small hydrocarbons in $CDCl_3$ at 25 °C show new signals at an extremely high field region which were assigned as the guest protons encapsulated within the cavity of H_2**CP**.

Thermodynamic data of the small hydrocarbon guests and H_2**CP** systems obtained from 1D-^{1}H NMR titrations are summarized in Table 1. The 1:1 association constants (K) were obtained from signal intensities of various concentrations of small hydrocarbon molecules in ^{1}H NMR spectra. Association constants between the host and each of the hydrocarbon guests show a clear correlation with the size of the guest molecules. Thermodynamic parameters including the standard free energy change ($\Delta G°$), the standard enthalpy change ($\Delta H°$), and the standard entropic change ($\Delta S°$), were obtained from van't Hoff plots generated from the data of ^{1}H NMR titrations at different guest concentrations and temperatures (25−45 °C). Negative $\Delta H°$ values for the present systems show that the encapsulated state is stabilized by host−guest interactions including van der Waals and CH/π interactions. Negative $\Delta S°$ values of these systems show that the encapsulation process destabilizes the systems as a result of the decreased mobility of guest molecules. In the guest encapsulation process, thermodynamic parameters for the desolvation of a guest molecule from a bulk solution should be taken into account for the evaluation of $\Delta S°$. In an aprotic and nonpolar solvent, the corresponding parameters for a gaseous small hydrocarbon molecule are small and the solvation energy will contribute less to them.[13] In the present systems, they are considered to be less than the experimental errors. By the cancellation of the two opposite effects, the encapsulation of small hydrocarbon molecules gives large negative $\Delta G°$ values. An increase in steric bulkiness causes a decrease in encapsulated-state stabilization. Acetylene has a higher affinity for the capsule, presumably because of the contribution of CH/π interactions of the acidic alkyne-H with the aromatic rings of the cavitand.

The perfect separation of signals with no peak broadening of free and encapsulated guest protons at 50 °C in the ^{1}H NMR spectra suggests that the guest exchange rates of these systems are slower than the ^{1}H NMR time scale. With the use of the normal pulse ^{1}H NMR program, the static parameters of these systems such as K, $\Delta G°$, $\Delta H°$, and $\Delta S°$ were found to correlate with the energy states before and after encapsulation, although the dynamic parameters such as guest exchange rates and activation energies correlating with the transition state cannot be obtained except for the relationship with the NMR time scale.

Association and Dissociation Rates Obtained from EXSY. Theoretically, kinetics of the association and dissociation processes of methane with H_2**CP** follow eq 1 with parameters including the second-order association rate constant (k_{ass}), the free-H_2**CP** concentration (H_{free}), the free-CH_4 concentration (G_{free}) concentration, the first-order dissociation constant (k_{diss}), and the concentration of the host−guest complex (H·G) (Scheme 1).

We measured 2D ^{1}H−^{1}H EXSY (NOESY) spectra of H_2**CP** with methane in $CDCl_3$ with a mixing time of 0.5 s at 25 °C (Figure 1). The spectrum clearly shows correlation cross peaks of magnetization exchange between the encapsulated methane and free methane.

(11) (a) Szabo, T.; Hilmersson, G.; Rebek, J., Jr. *J. Am. Chem. Soc.* **1998**, *120*, 6193. (b) Craig, S. L.; Lin, S.; Chen, J.; Rebek, J., Jr. *J. Am. Chem. Soc.* **2002**, *124*, 8780. (c) Scarso, A.; Onagi, H.; Rebek, J., Jr. *J. Am. Chem. Soc.* **2004**, *126*, 12728. (d) Cram, D. J.; Jaeger, R.; Deshayes, K. *J. Am. Chem. Soc.* **1993**, *115*, 10111.

(12) (a) Wik, B. J.; Lersch, M.; Krivokapic, A.; Tilset, M. *J. Am. Chem. Soc.* **2006**, *128*, 2682. (b) Scarso, A.; Rebek, J., Jr. *J. Am. Chem. Soc.* **2004**, *126*, 8956.

(13) Experimentally, the enthalpy of CH_4 dissolution in CCl_4 has been determined to be $\Delta H°_g$(298 K) = 1.54 $kcal\cdot mol^{-1}$ (Cone, J.; Smith, L. E. S.; Alexander van Hook, W. *J. Chem. Thermodyn.* **1979**, *11*, 277−285). The stabilization of methane by dispersion interaction in a gas phase is estimated to be −0.4 to −0.5 $kcal\cdot mol^{-1}$ by the calculation with aug(d,p)-6-311G** or aug(df,pd)-6-311G** bases sets (Tsuzuki, S.; Uchimaru, T.; Mikami, M.; Tanabe, K. *J. Phys. Chem. A* **1998**, *102*, 2091−2094). Thus, desolvation free energy ($\Delta G°_{desolv}$) in CCl_4 could not greatly deviate from ca. −1 $kcal\cdot mol^{-1}$ (=4 $kJ\cdot mol^{-1}$). Though the enthalpy data of CH_4 dissolution in $CDCl_3$ are not available, the values in CCl_4 and $CHCl_3$ would be similar, because the solubility of CH_4 into $CHCl_3$ (0.82 mL of CH_4/mL of $CHCl_3$ at 1 atm, 20 °C) is slightly less than that in CCl_4 (1.06 mL of CH_4/mL of CCl_4, at 1 atm, 25 °C) in consideration of similar nonpolar and aprotic halogenated solvents, see: Clever, H. L.; Young, C. L.; Battino, R.; Hayduk, W.; Wiesenburg, D. A. In *Solubility Data Series*; Clever, H. L., Young, C. L., Eds.; Pergamon Press: Oxford, UK, 1987; Vol. 27/28.

(14) ExsyCalc is available at http://WWW.mestrec.com/.

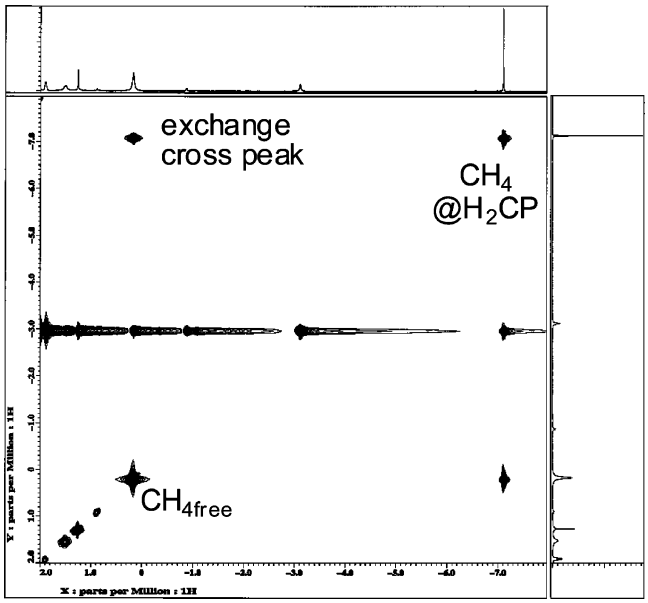

FIGURE 1. 2D-NOESY spectrum of the $CDCl_3$ solution of H_2**CP** (10 mM) with methane (5 mL bubbling by a syringe) with a mixing time of 0.5 s.

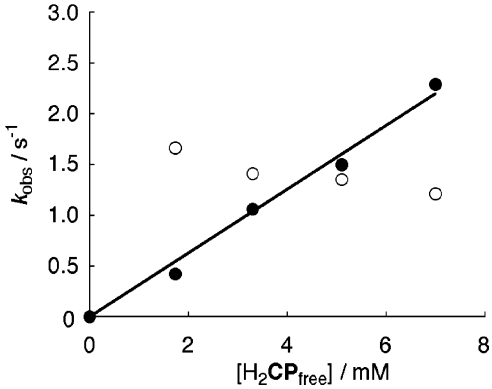

FIGURE 2. Relationship of k_{assobs} (filled circle) and $k_{dissobs}$ (open circle) with [H_2**CP**$_{free}$] for methane encapsulation in H_2**CP**. [$CH_{4\ free}$] ≈ 20 mM, [H_2**CP** $_{total}$] = 5, 10, 15, and 20 mM, in $CDCl_3$ at 25 °C.

From the intensities of the cross and diagonal peaks measured with mixing time 0 and 0.5 s, pseudo-first-order exchange rates between the two methane species (k_{assobs} and $k_{dissobs}$ displayed in eq 2) could be obtained by EXSY calculation software (ExsyCalc).[14] The values of k_{assobs} and $k_{dissobs}$ should follow pseudo-first-order kinetics as eq 3. Equation 4 was obtained from the relationship between eq 1 and eq 3. Thus, k_{ass} can be obtained from the plot of free host concentration vs k_{assobs}. k_{diss} could be almost the same value as $k_{dissobs}$ from eq 4. The plot of [H_2**CP**$_{free}$] vs k_{assobs} and $k_{dissobs}$ for methane encapsulation is shown in Figure 2. A linear correlation for k_{assobs} with free-H_2**CP** concentration was observed and $k_{dissobs}$ was found to be almost constant at ∼1.4 s^{-1}. This result provides support that the present kinetic analysis is correct. From the slope of k_{assobs} in Figure 2, the second-order association rate constant, k_{ass} = 320 M^{-1} s^{-1}, was obtained. From the obtained rate constants of methane exchange at 25 °C, the association constant K = 220 M^{-1} (=k_{ass}/k_{diss}) and the standard free energy change $\Delta G°$ = −13 kJ·mol^{-1} (=$-RT$ ln$K$) were calculated (Table 2). The $\Delta G°$ value was found to be essentially identical with the $\Delta G°$ value obtained from 1D NMR experiments ($\Delta G°$ = −10.9 kJ·mol^{-1}) in Table 1.

TABLE 2. Exchange Rates and Association Constants of Hydrocarbon Encapsulations in H_2CP at 25 °C Obtained by 2D EXSY[a]

	CH_4@H_2**CP**	C_2H_2@H_2**CP**	C_2H_4@H_2**CP**
k_{ass} (M^{-1}·s^{-1})	320	440	220
k_{diss} (s^{-1})	1.4	2.4	2.7
K (M^{-1})[b]	230	180	83
$\Delta G°$ (kJ·mol^{-1})	−13	−13	−11
$\Delta G^{‡}_{ass}$ (kJ·mol^{-1})[c]	59	58	59
$\Delta G^{‡}_{diss}$ (kJ·mol^{-1})[c]	72	71	71

[a] [H_2**CP**$_{total}$] = 10 mM, at 25 °C, in $CDCl_3$. Mixing time = 0.5 (CH_4), 0.25 (C_2H_2), and 0.3 s (C_2H_4). Pulse delay = 60 s. Estimated error range: k and K, <20%; $\Delta G°$, <5%. [b] $K = k_{ass}/k_{diss}$. [c] $\Delta G^{‡} = \{\ln(\kappa_B T/h) - \ln k\}/RT$, where κ_B and h are Boltzmann and Planck constants, respectively.

$$\frac{\partial[\mathrm{H{\cdot}G}]}{\partial t} = k_{ass}[\mathrm{H_{free}}][\mathrm{G_{free}}] - k_{diss}[\mathrm{H{\cdot}G}] \quad (1)$$

$$\mathrm{G_{free}} \underset{k_{dissobs}}{\overset{k_{assobs}}{\rightleftharpoons}} \mathrm{H{\cdot}G} \quad (2)$$

$$\frac{\partial[\mathrm{H{\cdot}G}]}{\partial t} = k_{assobs}[\mathrm{G_{free}}] - k_{dissobs}[\mathrm{H{\cdot}G}] \quad (3)$$

$$k_{ass}[\mathrm{H_{free}}] \approx k_{assobs}; \quad k_{diss} \approx k_{dissobs} \quad (4)$$

The association and dissociation rates of acetylene and ethylene into H_2**CP** were obtained by using the same method as for methane. The order of guest association rates of H_2**CP** was acetylene > methane > ethylene. This correlates with the association constant K obtained from the 1D NMR experiment. On the other hand, the order of dissociation rate constants (ethylene > acetylene > methane) correlates with the size of the guest molecules. Each association constant calculated from the exchange rate ($K = k_{ass}/k_{diss}$) is larger than the corresponding K values determined by 1D NMR. There is no apparent explanation for this difference. Some possibilities could include the differences in the 1D and EXSY methods and/or the deviation of the applied [H] and [G] from the conditions for an ideal pseudo-first-order kinetic measurement, which requires $[G]_o \ll [H]_o$. In this experiment, ideal pseudo-first-order conditions are difficult to ensure due to the solubility of the host in $CDCl_3$ and the lack of sufficient sensitivity to provide accurate integration of guest peaks and/or inaccuracies of the equations. Natural logarithmic treatment of the rate constants apparently decreases the errors of thermodynamic energies.

Comparison of Guest Exchange Rates for Various Capsule-Shaped Hosts. To compare the present guest exchange rate with those of reported capsule shaped host/small guest systems, standard activation free energy changes $\Delta G^{‡}$ were calculated at T = 298 K from the following eq 5, where κ_B and h are Boltzmann and Planck constants, respectively (Table 2).

$$\Delta G^{‡} = \frac{\ln(\kappa_B T/h) - \ln k}{RT} \quad (5)$$

The structure of reported capsule-shaped hosts, applied nonpolar guests, their association/dissociation rates, and their $\Delta G^{‡}$ values are shown in Table 3. In general, smaller $\Delta G^{‡}$ values give larger exchange rates. Activation free energies of the dissociation or exchange process were used for comparison. The

TABLE 3. Guest Exchange Rates and Activation Free Energies of Various Capsule Systems

Host	Guest	T; solvent	Rates	$\Delta G^{\ddagger}$, kJ·mol^{-1}	Ref.
Covalent-bonding type hosts					
H_2**CP**	CH_4	298 K; $CDCl_3$	k_{ass}= 320 $M^{-1}s^{-1}$ k_{diss}= 1.4 s^{-1}	$\Delta G^{\ddagger}_{diss}$ = 72	This work
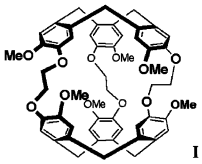 **I**	CH_4	298 K; $CDCl_3$	k_{diss}= 1.2 × 10^6 s^{-1}	$\Delta G^{\ddagger}_{diss}$ = 44	6e
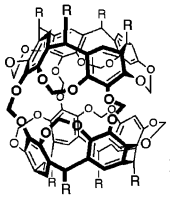 **II**	Xe	295 K; CD_2Cl_2	k_{ass}= 0.055 M^{-1} min^{-1} k_{diss}= 2.5 × 10^{-4} min^{-1}	$\Delta G^{\ddagger}_{diss}$ = 103	6b
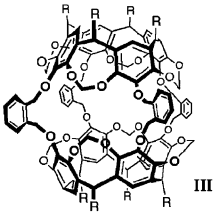 **III**	DMA	373 K; *o*-xylene-d_{10}	k_{ass} = 8.0 M^{-1} min^{-1} k_{diss} = 5.1 × 10^{-2} min^{-1}	$\Delta G^{\ddagger}_{diss}$ = 113	3d
Hydrogen-bonding type hosts					
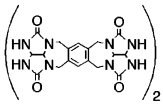 **IV**	C_2H_6	295 K; benzene-d_6	k_{ex} = 0.56 s^{-1}	$\Delta G^{\ddagger}_{ex}$ = 74	3a
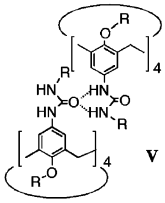 **V**	C_6H_6	298 K; benzene-d_6	k_{ex} = 0.47 s^{-1}	$\Delta G^{\ddagger}_{ex}$ = 75	8f
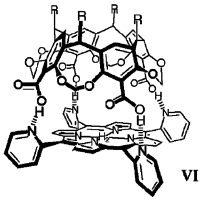 **VI**	ethylene	298 K; $C_2D_2Cl_4$	k_{ex}= 0.6 s^{-1}	$\Delta G^{\ddagger}_{ex}$ = 74	9c
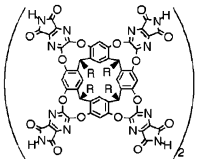 **VII**	benzene (co-guest: *p*-xylene)	295 K; *p*-xylene-d_{10}	k_{ex}= 0.25 s^{-1} (and 6.5 M^{-1} sec^{-1})	$\Delta G^{\ddagger}_{ex}$ = 76	8b

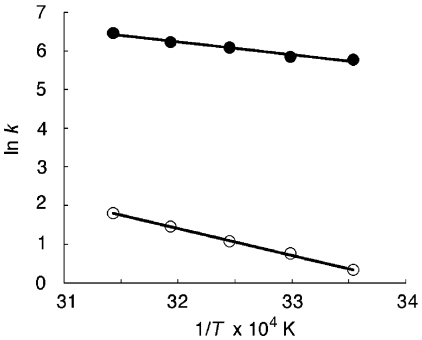

FIGURE 3. Arrhenius plots of k_{ass} (filled circle) and k_{diss} (open circle) for methane encapsulation in H_2**CP**. [$CH_{4\ free}$] ≈ 20 mM, [H_2**CP** $_{total}$] = 10 mM, in $CDCl_3$, in the range of 25−45 °C.

distribution of $\Delta G^{\ddagger}$ values for covalently linked host systems **I**−**III** spreads in a wide renge.[3b,c,6b,d,e] The rigid and fixed portal structure of covalently linked hosts may strongly affect the exchange rates which are dependent upon guest size. For example, the encapsulated Xe of system **II** cannot escape for several hours from the "hemi-carcerand" cavity, which has a very small portal ($\Delta G^{\ddagger}_{diss}$ = 103 kJ·mol). On the other hand, cryptphane-A in system **I** has large portals and easily releases methane within the NMR time scale ($\Delta G^{\ddagger}_{diss}$ = 44 kJ·mol). Thus, the reported examples belong to either of two extreme regions with respect to host association/dissociation rates. This is responsible for their *rigid* portal structures. However, H_2**CP** shows moderate rate constants for methane encapsulation. The dynamic structural change of its portal arising from the molecular flexibility of the host is a key for tuning of host association/dissociation rates.

In contrast, the hydrogen-bonding-type hosts in systems **IV**−**VII** show similar exchange rate constants to each other.[3a,8b,f,9c] The hydrogen bond cleavage rates of hosts determine the open and close rates of their capsule portals. Accordingly guest exchange rates of these systems fall into the same range (k_{ex} = 10^{-1} s^{-1} order, $\Delta G^{\ddagger}$ = 70−80 kJ·mol^{-1}).

The coalescence energy determined by peak separation of free and encapsulated guest in ^{1}H NMR was calculated to be about 63 kJ·mol^{-1} at room temperature.[6c] With the exception of the systems for which kinetic measurements were carried out, only 1D-^{1}H NMR spectra were measured to confirm encapsulation of guests.

From the kinetic measurement of methane exchange into H_2**CP** ($\Delta G^{\ddagger}_{diss}$ = 72 kJ·mol^{-1} at 298 K), we found that the exchange rate is similar to that of hydrogen bonding-type systems. The H_2**CP** system has moderate exchange rates to observe by NMR. This feature of H_2**CP** makes guest encapsulation occur easily. The moderate guest exchange rates of H_2**CP** observable by NMR are in a range suitable for catalytic applications. The information discussed above will be useful for the design of host molecules, which are capable of taking dynamic motion from their portal shape and sizes.

Activation Energy of Encapsulation. To obtain activation energies for the process of guest exchange, the temperature dependence of exchange rates was measured in the range of 25−45 °C. Arrhenius plots of the association and dissociation rates of methane encapsulation are shown in Figure 3. From the slope of the plots, the values of activation energies of association ($E_{a,ass}$) and dissociation ($E_{a,diss}$) processes were determined to be 27 and 58 kJ·mol^{-1}, respectively (Table 4). The difference between association and dissociation energy

TABLE 4. Thermodynamic Parameters of Hydrocarbon Encapsulation in H_2CP Obtained by 2D EXSY[a]

	CH_4@H_2**CP**	C_2H_2@H_2**CP**	C_2H_4@H_2**CP**
$\Delta G°$ (kJ·mol^{-1})[b]	−13	−13	−11
$\Delta H°$ (kJ·mol^{-1})[c]	−31	−35	−34
$\Delta S°$ (J·K^{-1}·mol^{-1})[d]	−60	−67	−77
lnA_{ass} (M^{-1}·s^{-1})[e]	17	20	16
lnA_{diss} (s^{-1})[e]	24	29	26
$E_{a,ass}$ (kJ·mol^{-1})[e]	27	34	27
$E_{a,diss}$ (kJ·mol^{-1})[e]	58	69	61
$\Delta G^{\ddagger}_{ass}$ (kJ·mol^{-1})[f]	59	58	59
$\Delta G^{\ddagger}_{iss}$ (kJ·mol^{-1})[f]	72	71	71
$\Delta H^{\ddagger}_{ass}$ (kJ·mol^{-1})[g]	25	31	25
$\Delta H^{\ddagger}_{diss}$ (kJ·mol^{-1})[g]	55	66	59
$\Delta S^{\ddagger}_{ass}$ (J·K^{-1}·mol^{-1})[h]	−113	−90	−118
$\Delta S^{\ddagger}_{diss}$ (J·K^{-1}·mol^{-1})[h]	−58	−16	−40

[a] [H_2**CP**$_{total}$] = 10 mM. Mixing time = 0.5 (CH_4), 0.25 (C_2H_2), and 0.3 s (C_2H_4). Pulse delay = 60 s. Error range: $\Delta G°$ and $\Delta G^{\ddagger}$, <5%; $\Delta H°$, $\Delta H^{\ddagger}$, ln A, and E_a, <10%; $\Delta S°$ and ΔS, <20%. [b] $\Delta G° = -RT \ln K$. [c] $\Delta H° = E_{a,ass} - E_{a,diss}$. [d] $\Delta S° = -(\Delta G° - \Delta H°)/T$. [e] Obtained by Arrhenius plots in the range of 25−45 °C. [f] $\Delta G^{\ddagger} = \{\ln(\kappa_B T/h) - \ln k\}/RT$, where κ_B and h are Boltzmann and Planck constants, respectively. [g] Obtained by Eyring plots in the range of 25−45 °C. [h] $\Delta S^{\ddagger} = -(\Delta G^{\ddagger} - \Delta H^{\ddagger})/T$.

corresponds to the standard enthalpy change $\Delta H° = -31$ kJ mol^{-1} (=$E_{a,ass}$− $E_{a,diss}$). The value shows a good correlation with the data obtained from 1D NMR measurements ($\Delta H° = -33$ kJ·mol^{-1}). The standard enthalpy change $\Delta S°$ (−63 J·K·mol^{-1}) was calculated from the abovementioned $\Delta G°$ (=$-RT \ln(k_{ass}/k_{diss})$) and $\Delta H°$ by $\Delta G° = \Delta H° - T\Delta S°$, where T = 298 K.

The activation enthalpy changes of association and dissociation, $\Delta H^{\ddagger}_{ass}$ (25 kJ·mol^{-1}) and $\Delta H^{\ddagger}_{diss}$ (55 kJ·mol^{-1}), were obtained from Eyring plots in the range of 25−45 °C, and the activation entropy changes of association, $\Delta S^{\ddagger}_{ass}$ (−113 J·K·mol^{-1}), and dissociation, $\Delta S^{\ddagger}_{diss}$ (−58 J·K·mol^{-1}), were calculated by $\Delta S^{\ddagger} = -(\Delta G^{\ddagger} - \Delta H^{\ddagger})/T$, where T = 298 K. The value $\Delta H^{\ddagger}_{ass}$ is the energy barrier when the guest methane molecule passes through the narrow portal of the capsule. The negative $\Delta S^{\ddagger}_{ass}$ and $\Delta S^{\ddagger}_{diss}$ values mainly indicate that the guest molecule is forced to decrease its molecular motion when it passes through the narrow portal of the host. Since the enthalpy change by desolvation of CH_4 in $CHCl_3$ is considered to be <4 kJ·mol, which is the same or less than the technical error of the present measurement, its contribution to the present thermodynamic evaluation can be ignored.[13] Corresponding activation energies for acetylene and ethylene encapsulation into the cavity were obtained in a similar manner. The thermodynamic parameters obtained for three guests show the following features:

(1) When the activation energies only represent the energy barrier of the guest into and out of the portal, the values will be the same. The activation energies for guest dissociation, $E_{a,diss}$, are about double those for association, $E_{a,ass}$. This reflects the degree of stabilization of the guest in the associated states.

(2) On the other hand, $E_{a,ass}$ does not reflect the stabilization of guests in the capsule and the values are almost equivalent in methane and ethylene, presumably because of the stabilization.

(3) The relatively less negative $\Delta S^{\ddagger}_{diss}$ value determined for acetylene could reflect the restriction of its movement in the cavity rather than the unbound phase. However, the $\Delta S^{\ddagger}_{ass}$ values for the three guests show only small differences. Since enthalpies of solvation/desolvation of guests in the solution are the same or less than the technical errors of the measurement, they can be ignored.

Overall, the observed thermodynamic parameters indicate the fine features of the process of encapsulation/dissociation by the

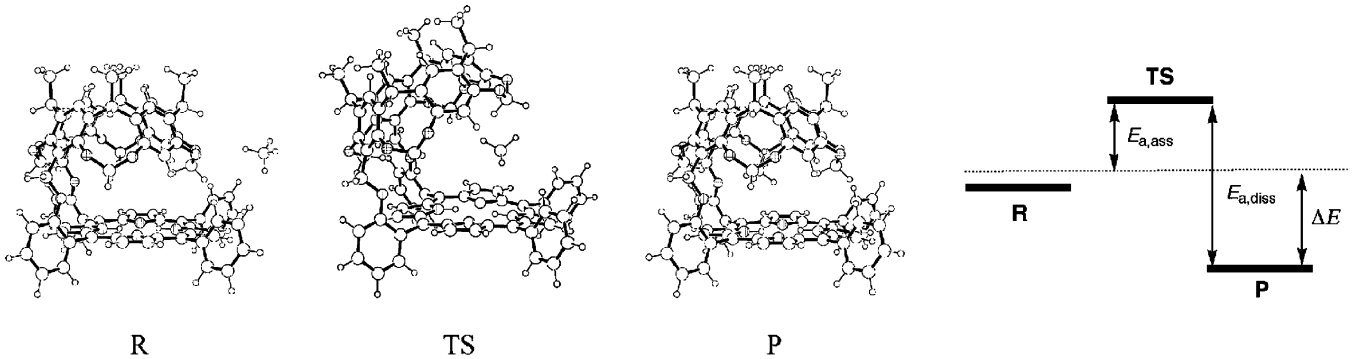

FIGURE 4. Stationary structures of the unbound state (**R**), transition state for encapsulation (**TS**), and the encapsulated state (**P**) of methane interaction with H_2**CP** at the theoretical level of HF/6-31G*. Their Cartesian coordinates are given in the Supporting Information (Tables S1−S3). The energy diagram was based on the state of two isolated monomers.

H_2**CP** host. This is the first example of comprehensive determination of activation energies experimentally in a capsule-shaped host/hydrocarbon guest system.

Methane Encapsulation Process Revealed by ab Initio MO Calculations. We obtained three stationary states for methane encapsulation: a local minimum corresponding to the methane unbound state (**R**), a transition state for methane encapsulation (**TS**), and a local minimum corresponding to the methane encapsulated state (**P**) at the theoretical level of HF/6-31G*. Note that methane is attached to the outside of porphyrin in the unbound state **R**. The energies of the three states, **R**, **TS**, and **P**, relative to the two isolated monomers were determined to be −2.54, 42.8, and 2.55 kJ·mol^{-1}, respectively. They were −8.17, 58.3, and −30.8 kJ·mol^{-1}, respectively, at MP2/6-31G**//HF/6-31G*. The MP2 method is needed to take dispersion energy into account, which is an essential factor for the stabilization of small hydrocarbons in the cavitand−porphyrin. The DFT method is not suited for this purpose, since most DFT methods cannot correctly take dispersion energy into account.[15] Actually, these values were calculated to be −7.17, 36.3, and −1.40 kJ·mol^{-1}, respectively, at B3LYP/6-31G**//HF/6-31G*. It is noteworthy that the large amount of stabilization of methane in the cavitand−porphyrin is ascribed to the dispersion energy, which can be taken into account with the MP2 method, but not with DFT.

The solvation effect is not taken into account in the current work. Qualitatively, this can be justified by considering that either the barrier of the encapsulation process or the stabilization in the cavitand−porphyrin is much larger than the interaction energy between methane and solvent molecules.

The structures of the stationary states are shown in Figure 4. Since the system of the cavitand−porphyrin associated with methane is very complex, there can be various local minima or transition states in the encapsulation process. The stationary states shown here can be regarded as the representative states. It is worthy to note that the structure of the methane encapsulated state (**P**) looks similar to that of the empty state (**R**) of the cavitand−porphyrin where the portal of the molecule is closed. In the transition state structure of the methane encapsulation process, the portal is open and a methane molecule is on the verge of entering or departing from the cavitand−porphyrin. The cavitand−porphyrin has the appearance of a jewel case with a hinge. The hinge is strong enough to store the jewel, a hydrocarbon.

(15) Johnson, E. R.; Wolkow, R. A.; DilLabio, G. A. *Chem. Phys. Lett.* **2004**, *394*, 334−338.

TABLE 5. Comparison of Energies Related to Methane Encapsulation in H_2CP from Experimental and MO Calculations[a]

	experiment		theory
	1D NMR R = CH_2CH_2Ph solvent $CDCl_3$	2D EXSY R = CH_2CH_2Ph solvent $CDCl_3$	MP2/6-31G**// HF/6-31G* R = CH_3 no solvent
$\Delta G°$ (kJ·mol^{-1})	−10.9	−13	NC[b]
$E_{a,ass}$ (kJ·mol^{-1})	−	27	$E_a = 58.3$
$E_{a,diss}$ (kJ·mol^{-1})	−	58	$E_a' = 89.1$
$\Delta H°$ (kJ·mol^{-1})	−33	−31	$\Delta E = -30.8$
$\Delta S°$ (kJ·mol^{-1})	−75	−60	NC[b]

[a] Relative energies are based on the two isolated monomer state. [b] Not calculated.

To obtain relative energies that take weak host−guest interactions into account, MP2/6-31G**//HF/6-31G* level calculations were carried out. The relative energy of the encapsulated state, −30.8 kJ·mol^{-1}, correlates well with the experimental $\Delta H°$, −31 kJ·mol^{-1}, which is the stabilization energy of the encapsulation state (Table 5). This can be interpreted partly as an accidental coincidence. The calculated activation energy, 58.3 kJ·mol^{-1}, is larger than the experimentally determined value of $E_{a,ass} = 27$ kJ·mol^{-1}. This difference is reasonable considering the fact that the potential energy surface is very flat both in the cavitand and in the vicinity of the **TS** state, which may indicate the high mobility of methane, and that the solvation effect is not taken into account in the theoretical investigation.

Conclusion

Guest exchange of capsule-shaped host molecules is the most fundamental dynamic process in host−guest chemistry. However, there are few examples reported of quantitative measurements of the exchange rates and activation energies of these systems. H_2**CP** has a flexible host structure and moderate affinity for guest molecules. It also demonstrates a completely isolated NMR signal of the entrapped state of the host molecule. This suggests that moderate guest exchange rates exist which are suitable for kinetic measurements by NMR. In this study, guest exchange rates (for association and dissociation) as well as thermodynamic parameters for encapsulation of three small hydrocarbon molecules were determined by EXSY to demonstrate good accordance of the values with those determined by 1D-^{1}H NMR. The observed activation energies for methane exchange at H_2**CP** were quantitatively compared to those of other host systems. Each of the covalent-bonded hosts, with

the exception of H_2**CP**, has a rigid portal structure designed to encapsulate small and escapable hydrocarbons. As a result, guest exchange rates are slow in solution at mild temperatures, relative to hydrogen bonding or metal coordinating systems. A host with a moderate guest exchange rate is capable of retaining a guest molecule in its cavity for a certain time: e.g. the half-life of entrapped CH_4 in H_2**CP** is 0.5 s. This is a sufficient period for completion of various types of reactions in the cavity. In the present cavitand porphyrin, the corresponding metal derivatives, M**CP**s, will be good candidates for further examination of catalytic reactions of encapsulated guests. The present kinetic and thermodynamic parameters will provide the fundamental knowledge for design of reactions of small hydrocarbons in M**CP**.

Experimental Section

General. Synthesis and characterization of H_2**CP** were reported in our previous paper.[9b] $CDCl_3$ and guest hydrocarbon gases were used as received without further purification. NMR spectra were recorded on a 500 MHz spectrometer. ^{1}H NMR chemical shifts (δ) are reported in parts par million (ppm) relative to TMS, using the residual proton resonance of $CDCl_3$ ($\delta = 7.26$ ppm).

EXSY Spectroscopy. H_2**CP** was dissolved in $CDCl_3$ (10 mM, 0.7 mL). Then, guest molecules in the gaseous state were directly bubbled into a gastight NMR tube with a valve. 2D EXSY spectra were recorded with use of a NOESY pulse program (noesy). All spectra were recorded at 500.13 MHz with 256 × 128 data points, a mixing time of 0.5 s for methane, 0.25 s for acetylene, and 0.3 s for ethylene, and a mixing time of 0 s for reference, a relaxation delay of 30 s for enough T_1 relaxation of guests in the condition (τ of guests <10 s), times = 16, for 10 ppm range at 25−45 °C. The basis for the extraction of kinetic and thermodynamic data produced by the EXSY experiments is integration of the cross peaks on the 2D NMR spectra. Magnetization exchange rates were obtained from cross and diagonal peak intensities, using ExsyCalc software.[14]

MO Calculations. The geometries of CH_4, H_2**CP**, and CH_4@H_2**CP** were optimized at the HF/6-31G* level of theory under solvent-free conditions. For the core of the cavitand porphyrin, the X-ray crystallographic data of Zn**CP** were used as the initial coordinates of the cavitand−porphyrin host molecule.[9b] Four phenylethyl groups at the rim of the cavitand are simplified and replaced by methyl groups and free base was used instead of the Zn complex. The transition state (TS) structure along the hydrocarbon encapsulation reaction coordinate was determined for CH_4@H_2**CP**. Intrinsic reaction coordinate (IRC) calculations were also performed at the same level of theory. Local minima and TS structures were identified by a full analysis of the vibrational modes, using analytical second derivatives of HF/6-31G*. The electron correlation energy corrections were added to the interaction energies according to the Møller−Plesset theory, truncated at the second-order (MP2) with the 6-31G** basis set for local minima and TS structures determined at HF/6-31G*: i.e., MP2/6-31G**//HF/6-31G* calculations were performed. B3LYP/6-31G**//HF/6-31G* calculations were also performed. The program package Gaussian03[16] was used for all ab initio MO calculations.

Acknowledgment. This work was supported by the Grants-in-Aid for Scientific Research (A)/(S) (17105003) and for Exploratory Research (18655072) from JSPS as well as by a grant from The Asahi Glass Foundation. J.N. acknowledges a JSPS Research Fellowship.

Supporting Information Available: Tables S1−S3 giving atom coordinates for the theoretical calculation of **R**, **T**, and **P** states. This material is available free of charge via the Internet at http://pubs.acs.org.

JO701299V

(16) Frisch, M. J.; et al. *Gaussian 03*, Revision C.02; Gaussian, Inc.: Wallingford, CT, 2004.